



Universidade de Brasília - UnB
Faculdade UnB Gama - FGA
Gas Dynamics

Analitical Calculations for a Supersonic Diffuser and Nozzle

Luso de Jesus Torres

Brasília, DF
2021



Contents

1	INTRODUÇÃO	3
I	PLANAR SUPERSONIC DIFFUSER	4
2	GEOMETRY DESCRIPTION	5
3	SHOCK WAVE THEORY	6
3.1	Shock Wave Description	6
3.2	Governing Equations	7
3.2.1	Normal Shock Wave	7
3.2.2	Oblique Shock Wave	9
4	METHODS	12
5	RESULTS OF PART I	13
II	CONICAL AND BELL-SHAPED NOZZLES	17
6	GEOMETRY DESCRIPTION	18
7	NOZZLE THEORY	19
7.1	Governing Equations	20
7.1.1	Heat Addition	20
7.1.2	Equation System for One-Dimensional Flow	20
7.1.3	Convergent-Divergent Nozzle	21
8	METHODOLOGY	22
9	RESULTS OF PART II	23
10	CONCLUSION	30
	REFERENCES	31
	ANNEX	32
	ANNEX A – DIFFUSER DESIGN	33

ANNEX B – NOZZLE DESIGN	37
ANNEX C – BELL-SHAPED PARAMETERS	42
ANNEX D – CONICAL-SHAPED PARAMETERS	45

1 Introdução

The present work pursues to find the optimal geometry for a planar supersonic diffuser with a given configuration with minimal total pressure losses in part I and analyze analytically flow in a conical versus bell-shaped nozzles using the results obtained as part II.

Part I

Planar Supersonic Diffuser

2 Geometry Description

The supersonic diffuser proposed is designed to work with maximum efficiency at Mach 3.5 and an equivalent altitude of 22 km in this specific case. Figure 1 shows the intended configuration. The geometry is basically described by two angles (θ_1 and θ_2) which will be responsible for changing the flow direction in this diffuser.

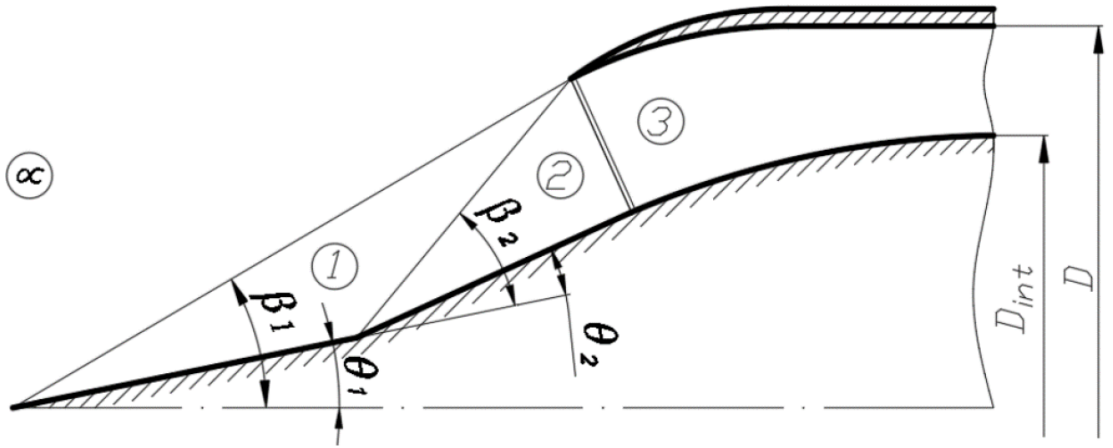


Figure 1 – Supersonic Diffuser Geometry

As a result from encountering the walls of the diffuser with an angle θ_1 , the free-stream flow will generate an oblique shock wave with an angle β_1 and subsequently generate volume 1 (LIEPMANN; ROSHKO, 2001). The same process will occur again with the angle change θ_2 , generating another oblique shock wave with angle β_2 , followed by a flow region 2. Further on, is intended a normal shock wave in front of the outer wall of the diffuser, generating the flow region number 3.

The subsequent sections will describe and calculate five properties of the flow in each region given the relations of these and other parameters, namely: Mach Number, static Pressure, Temperature, Velocity and Density. Drag also will be evaluated per unit span for the case of a wedge diffuser.

3 Shock Wave Theory

3.1 Shock Wave Description

Disturbances created in a fluid by a moving body are propagated or communicated to other parts of the fluid. The motion of the disturbances relative to the fluid is called wave motion, and the speed of propagation is called wave speed. When the flow velocity is supersonic, the wave motion cannot work its way upstream, and as a result, the disturbance waves pile up and coalesce, forming a standing wave in front of the body, that is called a shock wave (LIEPMANN; ROSHKO, 2001).

Shockwave is an extremely thin region, normally of the order of 10^{-5} cm, across which the flow properties can change drastically (ANDERSON, 2010). The shock wave is usually at an oblique angle to the flow (Figure 2a), however there are many cases where there are some interest in a shock wave normal to the flow (Figure 2b). A shock wave is nearly an explosive compression process, where the pressure increases almost discontinuously across the wave, associated with high irreversibility in the process.

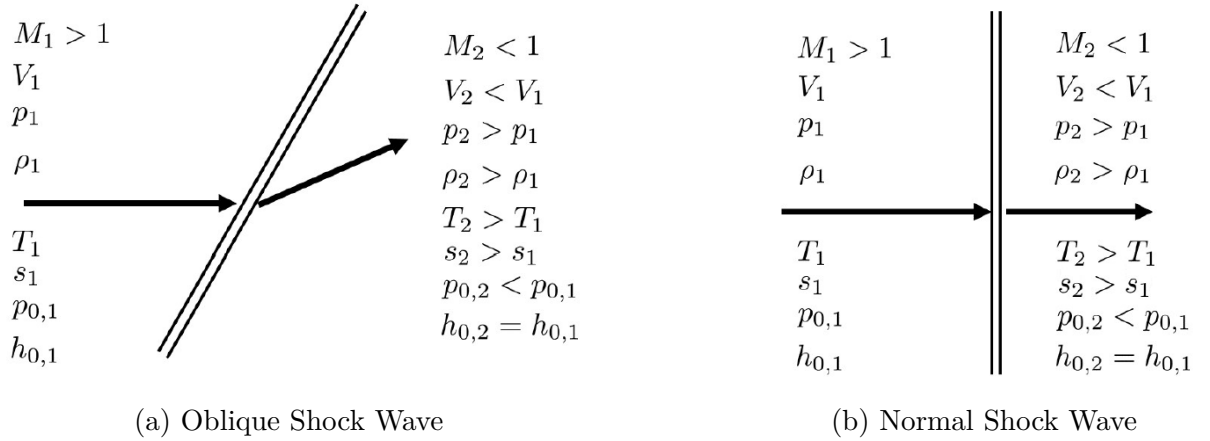


Figure 2 – Shock Wave Configurations

To the rest of the work, properties which are located behind the wave will be designated with the subscript “1”, and for the the properties after the wave, the subscript “2”, as shown in Figures 2a and 2b. For posterior regions, the subscripts will follow the sequence 3, 4... as needed.

3.2 Governing Equations

The following equations are essential to determine the optimal value of the diffuser for the given configuration, and to apply to this context, is important to remember some of the assumptions made by these results ([ANDERSON, 2010](#)):

- Steady flow (all properties stay constant with respect to time intervals);
- Adiabatic flow (all the processes taken here have no heat transfer between the flow and the surroundings);
- No viscous effects (no dissipative effects related to friction or molecular forces);
- No body forces (potential energy terms can be neglected);
- Calorically perfect gas (constant specific heats; enthalpy and internal energy are only functions of temperature);

3.2.1 Normal Shock Wave

As previously discussed, Normal Shock Wave can be considered as an specific case of the oblique shock wave, but for instructional purposes, it will be given in different topics.

Pressure

The ratio between the pressures before and after the wave is given by ([ANDERSON, 2010](#)) as:

$$\frac{P_2}{P_1} = 1 + \left(\frac{2\gamma}{\gamma + 1} \right) (M_1^2 - 1) \quad (3.1)$$

where

- P describes the static pressure;
- γ describes the heat capacity ratio or adiabatic index of the gas ($\gamma = 1.4$ for air);
- M describes the Mach Number.

Density

The ration between densities before and after the shock wave is given as:

$$\frac{\rho_2}{\rho_1} = \frac{(\gamma + 1)M_1^2}{2 + (\gamma - 1)M_1^2} \quad (3.2)$$

where

- ρ describes the density.

Temperature

The ratio of temperatures before and after the shock wave:

$$\frac{T_2}{T_1} = \frac{P_2}{P_1} \frac{\rho_1}{\rho_2} \quad (3.3)$$

where

- T describes the temperature.

Entropy

The entropy change across the shock wave is given by:

$$\Delta s = c_p \ln \left[\left(1 + \frac{2\gamma}{\gamma + 1}(M_1^2 - 1) \right) \frac{2 + (\gamma - 1)M_1^2}{(\gamma + 1)M_1^2} \right] - R \ln \left(1 + \frac{2\gamma}{\gamma + 1}(M_1^2 - 1) \right) \quad (3.4)$$

where

- Δs describes the net change in entropy;
- c_p describes the specific heat for constant pressure;
- R describes the gas constant ($R = 287 \text{ J kg}^{-1} \text{ K}^{-1}$ for air).

For a specific value of $M < 1$, Equation 3.4 states that *the shock wave phenomena impossible to take place*. Otherwise, it would violate the second law of thermodynamics, since for this situation, $\Delta s < 0$.

Another important result that comes from c_p is the relation (ANDERSON, 2010):

$$c_p = \frac{\gamma R}{\gamma - 1} \quad (3.5)$$

Total Pressure

The ratio of total pressures before and after the shock wave is given by:

$$\frac{p_{0,2}}{p_{0,1}} = \exp\left(\frac{-\Delta s}{R}\right) \quad (3.6)$$

where

- p_0 describes the total pressure.

It is important to remember the value behind the equation 3.6, which states that the total temperature stay constant throught the shock, but there are losses in the pressure across it.

Mach Number

The Mach number has a special relationship across the wave:

$$M_2^2 = \frac{1 + [(\gamma - 1)/2]M_1^2}{\gamma M_1^2 - (\gamma - 1)/2} \quad (3.7)$$

Speed of Sound

The speed of sound for a perfect gas can be expressed as:

$$a = \sqrt{\gamma RT} \quad (3.8)$$

where

- a describes the speed of sound.

The relation of speed of sound with the Mach number is given by:

$$M = \frac{V}{a} \quad (3.9)$$

where

- V describes the flow velocity

3.2.2 Oblique Shock Wave

The geometry of an oblique shock wave involves one more parameter when compared to the normal shock, which is the angle associated with the concave corner θ (Figure 3).

θ - β - M Relation

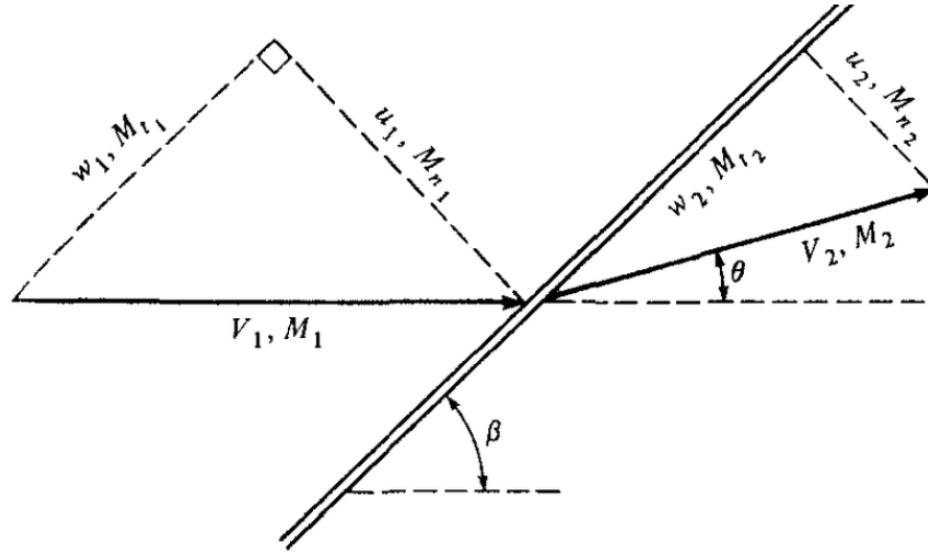


Figure 3 – Oblique Shock Parameters

The angles θ , β and the Mach Number M_1 are responsible for the shock wave obtained from a flow, and for specific design considerations, the following expression describes the so called $\theta - \beta - M$ relation:

$$\tan \theta = 2 \cot \beta \left(\frac{(M_1^2 \sin^2 \beta) - 1}{M_1^2 (\gamma + \cos 2\beta) + 2} \right) \quad (3.10)$$

Normal Component M_n

Another relation resultant from Figure 3 is the relation of the normal and the oblique shock:

$$M_{n,1} = M_1 \sin \beta \quad (3.11)$$

In the equation 3.11, $M_{n,1}$ represents the normal component of the Mach number M_1 , and from equation 3.7, the following relation between Mach numbers is obtained:

$$M_{n,2}^2 = \frac{1 + [(\gamma - 1)/2] M_{n,1}^2}{\gamma M_{n,1}^2 - (\gamma - 1)/2} \quad (3.12)$$

And after the shock the relation is:

$$M_2 = \frac{M_{n,2}}{\sin (\beta - \theta)} \quad (3.13)$$

Total Efficiency

Finally, considering the total loss present on the diffuser, we can evaluate the total efficiency in terms of pressure as:

$$\frac{p_{0,4}}{p_{0,1}} = \frac{p_{0,4}}{p_{0,3}} \frac{p_{0,3}}{p_{0,2}} \frac{p_{0,2}}{p_{0,1}} \quad (3.14)$$

Drag

To evaluate the drag, the concept of a wedge surface will be considered as the geometry shape. Figure 4 shows the acting forces.

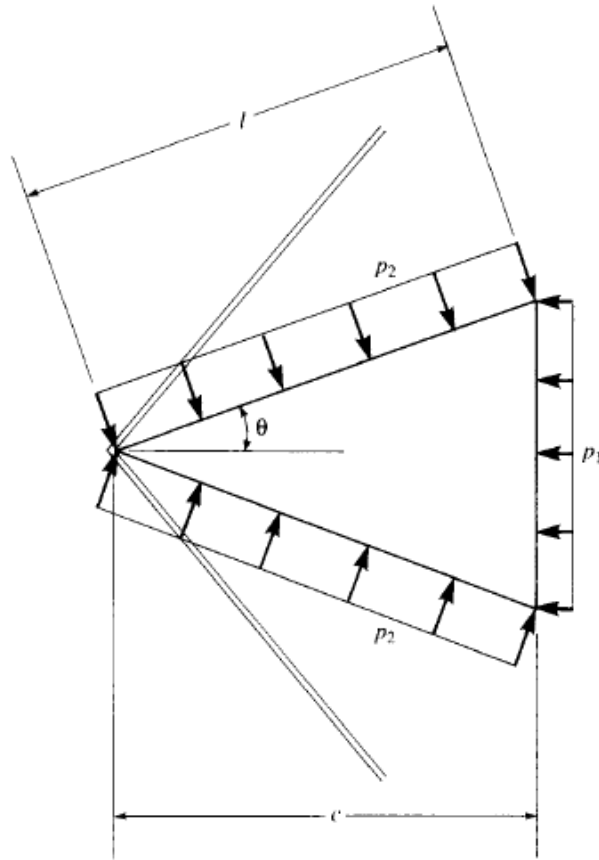


Figure 4 – Drag generated over a Wedge surface.

The drag generated, also called wave drag ([ANDERSON, 2010](#)), is evaluated as follows:

$$D = 2 l \sin \theta (p_2 - p_1) \quad (3.15)$$

For both sections, we obtain:

$$D = 2 l_1 \sin \theta_1 (p_2 - p_1) + 2 l_2 \sin \theta_2 (p_3 - p_2) \quad (3.16)$$

4 Methods

A diffuser is a device for reducing an incoming fluid flow to lower velocities with minimal losses in static pressure.

In the ideal case, such deceleration would be isentropic, but as explained in shock wave theory section, there will be always a certain loss due to the non-isentropic nature of the shock wave. Nevertheless, it is possible to obtain the optimized geometry, given the set of equations and properties in the inlet. To do so, a variable called “Pm” was created to quantify the total pressure ratio $\left(\frac{P_{0,i}}{P_{0,e}}\right)$ with the attempt to maintain it closer to 1.

The results are shown in the next chapter and the appendix containing the code can be found in Annex [A](#).

5 Results of Part I

To summarize results, Table 1 resumes the values calculated by the program with the equations developed. For the obtained geometry, Table 2 resumes the values obtained to match the theory.

The nomenclature of the stations adopted followed the order 0 to 3 being the free-stream region the first station and the sequence given by the exposed in the diffuser representation (Fig. 1).

The step chosen to obtain the optimal geometry corresponded to 0.1° , starting from 1° until 89° . The following graphs (Figs. 6 to 10) represent the ascending or descending behavior of each property by stage.

For the data obtained, the optimal geometry of the diffuser illustrated in Fig. 5 sketched in CATIA V5R19.

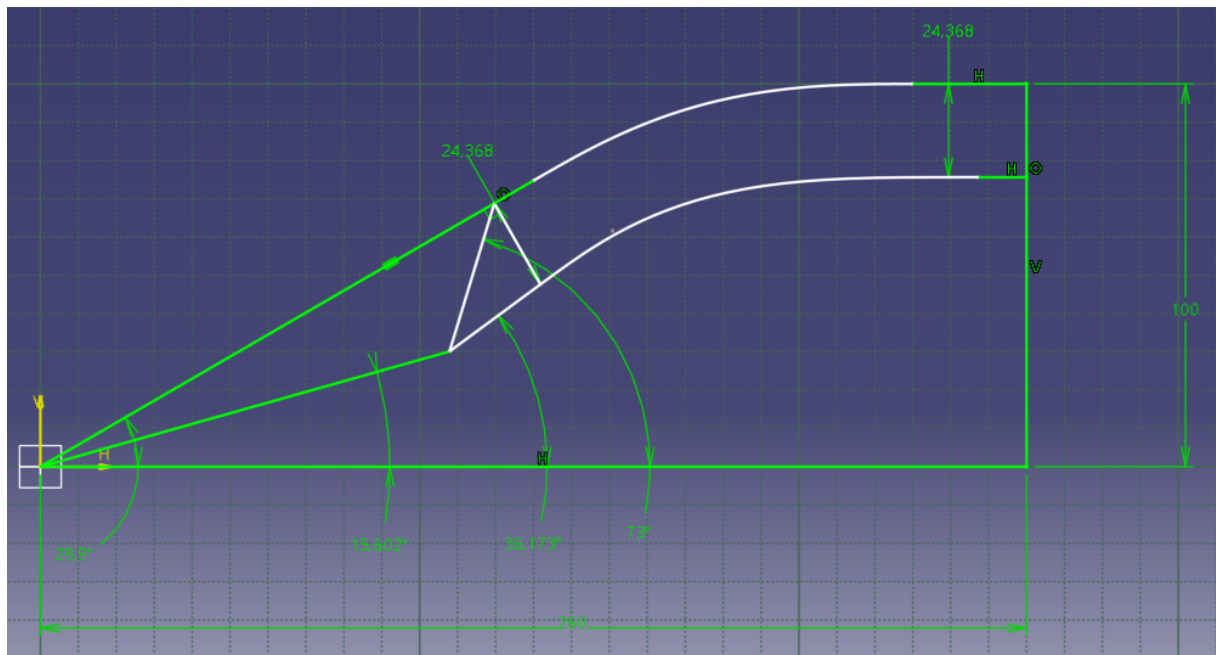


Figure 5 – Diffuser Design [mm]

Parameter \ Station	0 (∞)	1	2	3
Mach Number	3.5	2.55	1.65	0.66
Static Pressure [kPa]	5.47	18.58	63.02	189.12
Temperature [K]	216.65	325.82	489.97	701.21
Velocity [km/s]	1.03	0.93	0.73	0.35
Density [kg/m ³]	0.09	0.20	0.45	0.94

Table 1 – Design Parameters for each Station

Property	Value
$\beta_1 [deg]$	29.90
$\beta_2 [deg]$	43.10
$\theta_1 [deg]$	15.60
$\theta_2 [deg]$	20.57
$\left(\frac{P_{0,e}}{P_{0,i}}\right)$	0.62
D [kN]	1716.5

Table 2 – Expected angles, efficiency and Drag

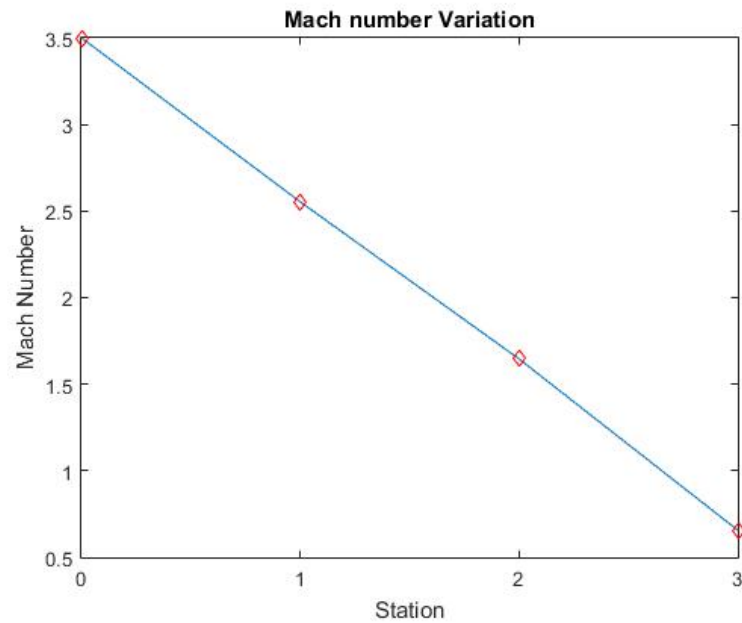


Figure 6 – Mach Number along the Stations

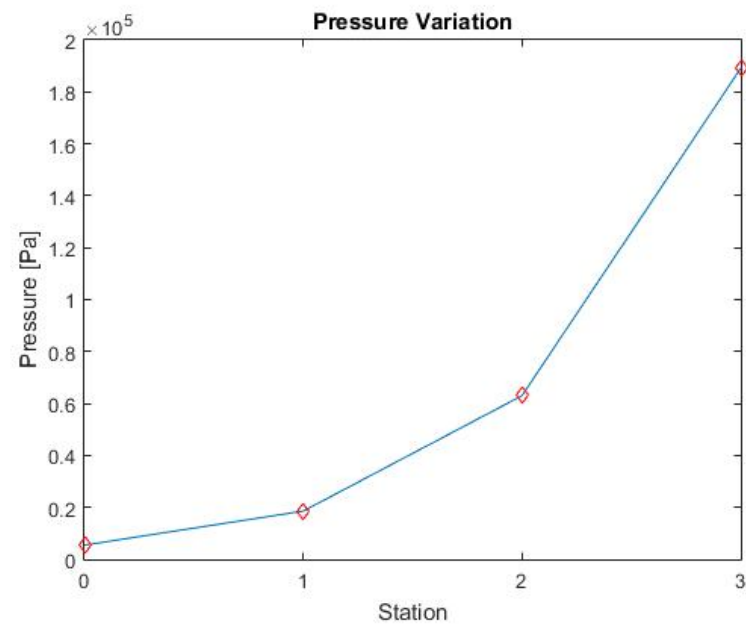


Figure 7 – Pressure along the Stations

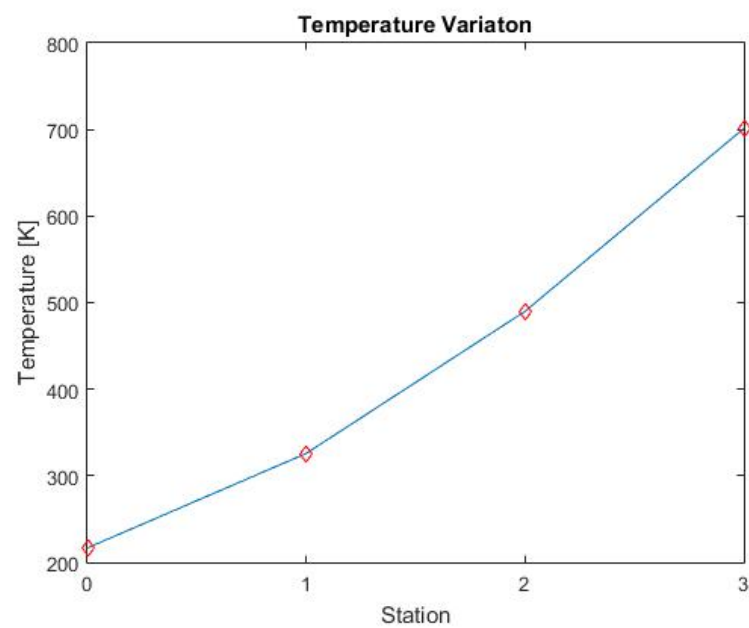


Figure 8 – Temperature along the Stations

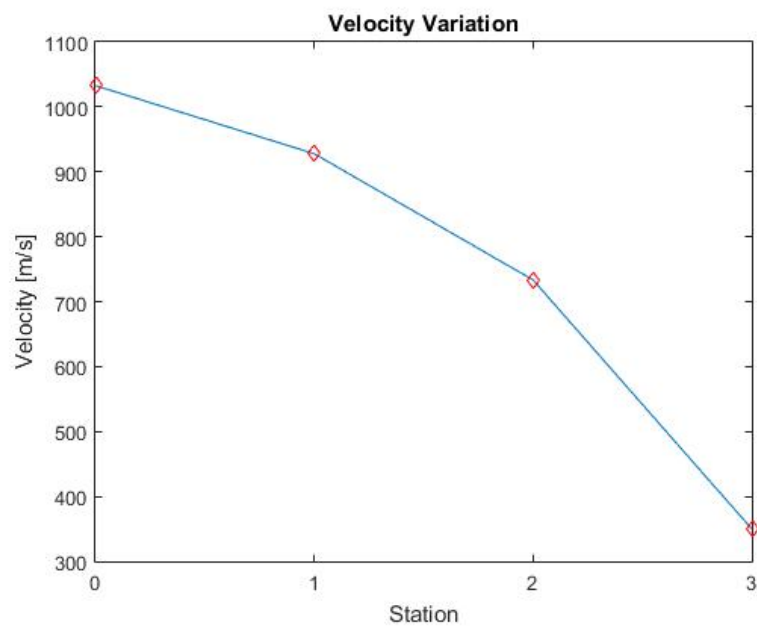


Figure 9 – Velocity along the Stations

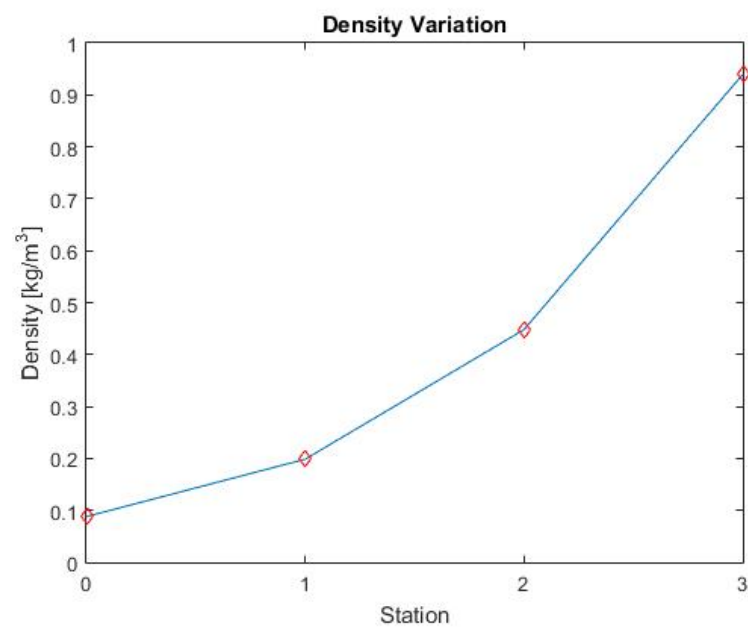


Figure 10 – Density along the Stations

Part II

Conical and Bell-Shaped Nozzles

6 Geometry Description

To complement the first part, where we develop a diffuser with optimal characteristics at the altitude of 22 km and Mach Number 3.5, in this part, two different configurations of ramjet nozzles will be compared. Fig. 11 shows the geometry to be discussed.

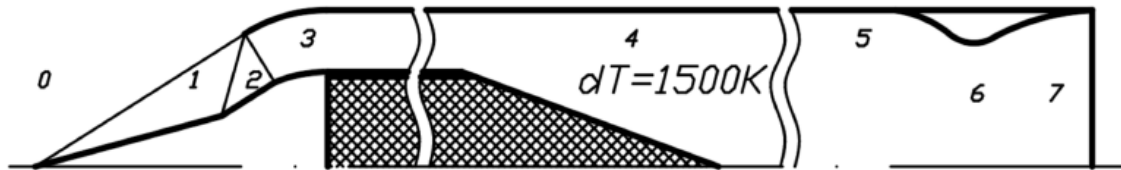


Figure 11 – RAMJET to be considered

The subsequent sections will be devoted to present the governing equation systems and discover the best shape for this specific work.

In the Previous part, the stations 0, 1, 2 and 3 were components of the diffuser part of the motor. volume 4 represents the combustion chamber (in the calculations will be only evaluated as heat addition) and the effect of flow expansion and finally for 5 to 7 can be observed the nozzle.

To the purpose of this part, the heat addition will yield a heat variation equivalent to 1000K. Further on, the air will be analyzed to the conic and bell shaped geometries.

7 Nozzle Theory

Considering a supersonic flow inside a duct, is important to consider some other effects and how the flow changes beyond shock waves, such as friction and heat addition (ANDERSON, 2010). This is a governing phenomenon in turbojet and, our study object, ramjet engine burners, where the heat is added in the form of fuel-air combustion.

To determine the geometric properties and the best shape of our geometry is to analyze the theory of Nozzles and Diffusers (ANDERSON, 2010). As a way to clarify some applications of this theory, Fig. 12 resumes the regions the DeLaval Nozzle (CLARKE; CARSWELL, 2007), where some of the elements will not be considered here, such as the viscous boundary layer and the combustion chamber region.

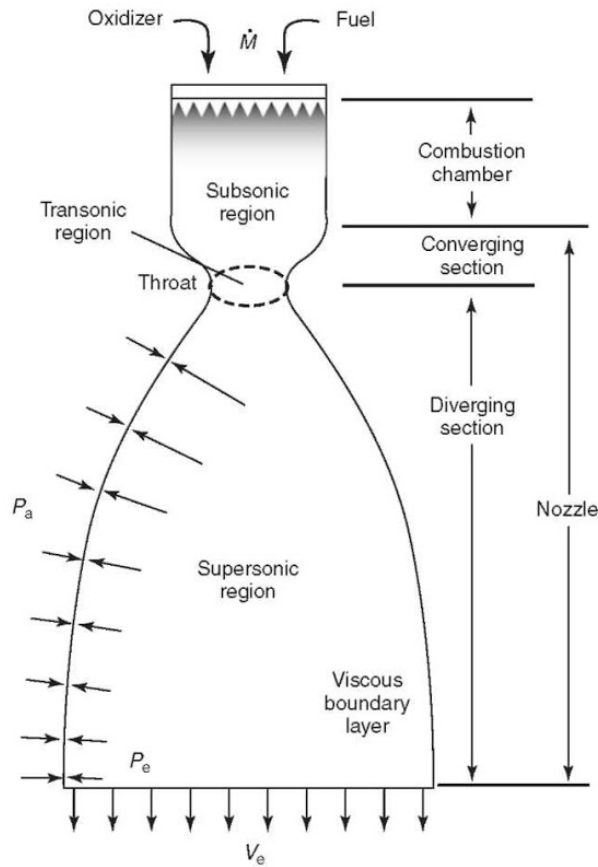


Figure 12 – DeLaval Nozzle. Source: (CLARKE; CARSWELL, 2007)

As labeled in the illustration of the nozzle, there are three specific regions of interest, being the converging section, the transonic region and the diverging region. In the entrance, the flow of gases is accelerated along with the converging portion of the nozzle (ANDERSON, 2010), where at the throat (known as the region with the minimal transverse area of the device), the flow reaches sonic speed ($Mach = 1$). After crossing the

throat, the diverging part of the nozzle takes place, where now the fluid can be accelerated to the exit with supersonic speeds.

As previous said, this device is present in a wide range of configurations and for this specific work will be a component of a ramjet motor, which with the data obtained from part one, will be designed in a bell or conic-shaped geometry as well as the properties in its exit.

7.1 Governing Equations

Three fundamental concepts are discussed in this section: Heat Addition and the set of isentropic relations for Quasi-one-dimensional Flow ([ANDERSON, 2010](#)).

7.1.1 Heat Addition

To model the heat addition, we must consider the energy equation, which for a calorically perfect gas results in:

$$q = c_p(T_{0,2} - T_{0,1}) \quad (7.1)$$

Equation 7.1 states that *the effect of heat addition directly changes the total temperature of the flow*.

7.1.2 Equation System for One-Dimensional Flow

For the computation of the effects of heat addition in the remaining properties, the following set of equations dictates the isentropic relations and were previously discussed in Normal Shock Wave Theory (section 3.2.1).

Ratio of Densities

$$\frac{\rho_2}{\rho_1} = \frac{(\gamma + 1)M_1^2}{2 + (\gamma - 1)M_1^2} \quad (7.2)$$

Ratio of Pressures

$$\frac{p_2}{p_1} = \frac{1 + \gamma M_1^2}{1 + \gamma} \quad (7.3)$$

$$\frac{p_{0,2}}{p_{0,1}} = \frac{1 + \gamma M_1^2}{1 + \gamma M_2^2} \left(\frac{1 + (\gamma - 1)M_2^2/2}{1 + (\gamma - 1)M_1^2/2} \right)^{\frac{\gamma}{\gamma - 1}} \quad (7.4)$$

Ratio of Temperatures

$$\frac{T_2}{T_1} = \left(\frac{1 + \gamma M_1^2}{1 + \gamma M_2^2} \right) \left(\frac{M_1}{M_2} \right)^2 \quad (7.5)$$

$$\frac{T_{0,2}}{T_{0,1}} = \frac{1 + \gamma M_1^2}{1 + \gamma M_2^2} \left(\frac{1 + (\gamma - 1)M_2^2/2}{1 + (\gamma - 1)M_1^2/2} \right) \left(\frac{1 + (\gamma - 1)M_2^2/2}{1 + (\gamma - 1)M_1^2/2} \right) \quad (7.6)$$

7.1.3 Convergent-Divergent Nozzle

The differential form of the continuity equation for the Quasi-One-dimensional flow give us the area-velocity relation ([ANDERSON, 2010](#)):

$$\frac{dA}{A} = (M^2 - 1) \frac{du}{u} \quad (7.7)$$

Hence, for:

- $0 \leq M < 1$ (subsonic flow) - Equation 7.7 yields an increase in velocity for convergent flow and decrease in velocity for a divergent duct.
- $M > 1$ (supersonic flow) - Equation 7.7 relates an increase in velocity corresponding to an increase in the transverse area of the nozzle, and a decrease in velocity for a convergent duct.
- $M = 1$ - In this situation, Equation 7.7 indicates for which area the transition between subsonic region and supersonic region will occur, where the local area of the device has its minimal value inside the nozzle or diffuser. This area is also called the *throat*.

Ratio of Areas in the Nozzle

The relation between the area with the Mach number is described by equation 7.8, where for a specific Mach Number, it is possible to evaluate which throat area will be responsible to accelerate our flow.

$$\left(\frac{A}{A^*} \right)^2 = \frac{1}{M^2} \left[\frac{2}{\gamma + 1} \left(1 + \frac{\gamma - 1}{2} M^2 \right) \right]^{\frac{\gamma + 1}{\gamma - 1}} \quad (7.8)$$

For this work, the ratio $\frac{A}{A^*} \geq 1$ produce the supersonic flow at the exit of the nozzle, so, to satisfy this relation, volume 5 represents the subsonic part of the nozzle (the convergent region), volume 6 represents the throat and finally volume 7 represents the supersonic divergent region.

8 Methodology

To evaluate the expansion of volume 3 to volume 4, we must use equation 7.8 to identify the correspondent area for the Mach Number at volume 3. The steps of calculation for M4 are done by the use of the function *fzero* from MATLAB in the main code, where it was used to match the values between the equality in equation 7.8. To calculate the respective properties of the flow, equations 7.2 to 7.5 will be used.

The corresponding properties for the remaining volumes can be obtained in terms of the isentropic relations developed to Normal Shock Waves, and for volumes 5 to 7 all parameters will be represented as a function of the position(Annex B).

To ease the understanding of the code, two additional parts were made separately and are responsible to quantify both analyzed geometries (Annex C and D).

9 Results of Part II

The following parameters and graphs were obtained with the MATLAB script in Annex B.

For the bell-shaped nozzle, Figures 13 to 15 shows the results obtained. In the case of the conical-shaped nozzle, Figures 16 to 18 illustrate the obtained.

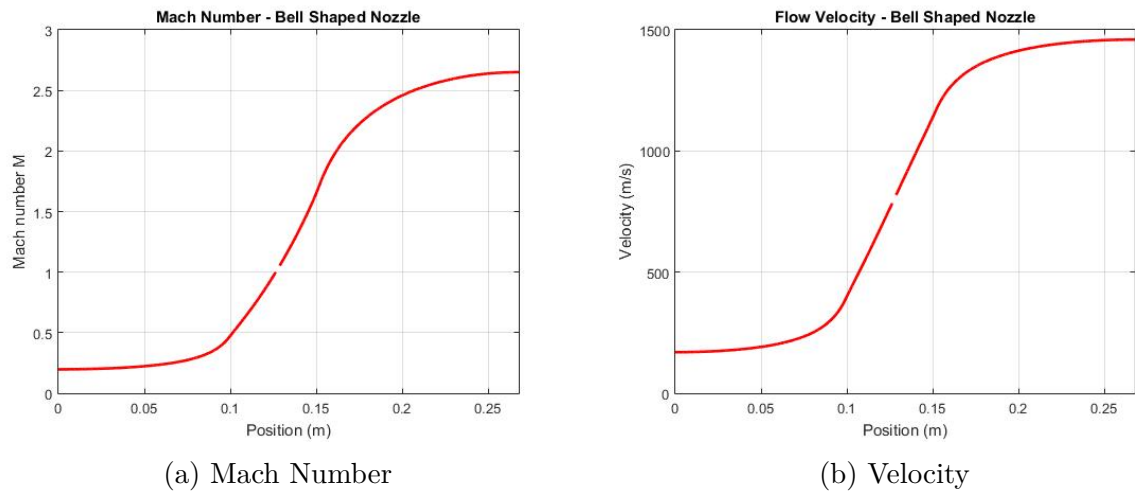


Figure 13 – Bell-Shaped Parameters 1

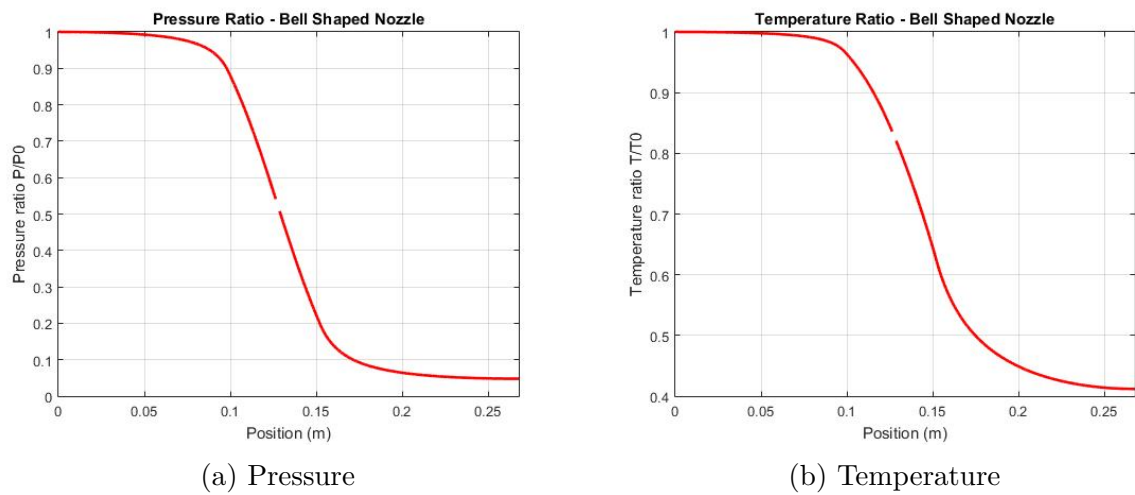
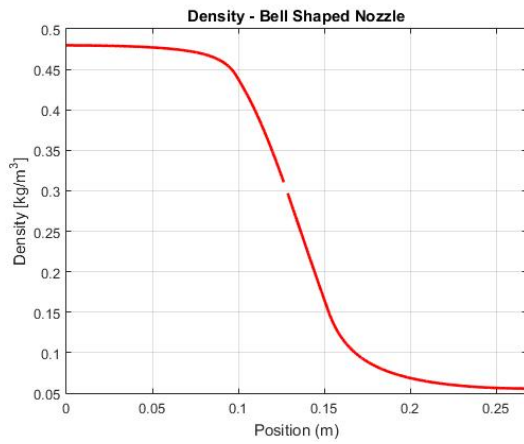
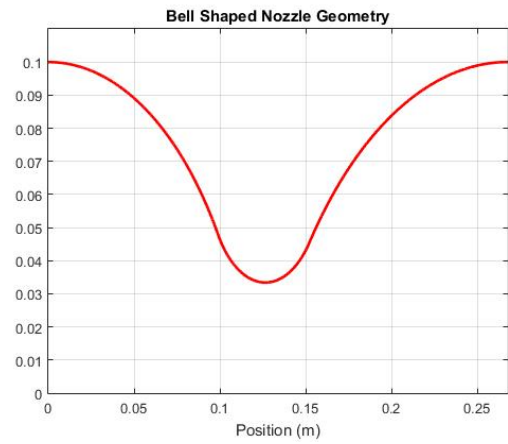


Figure 14 – Bell-Shaped Parameters 2

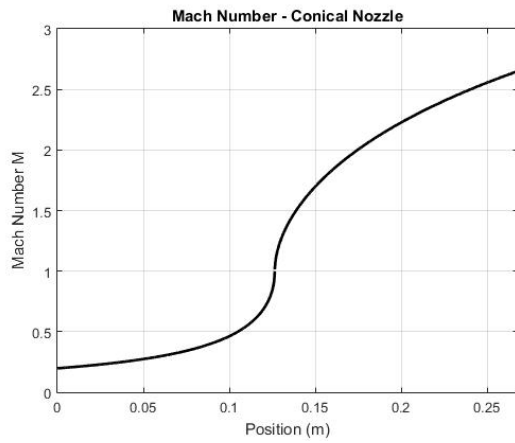


(a) Density

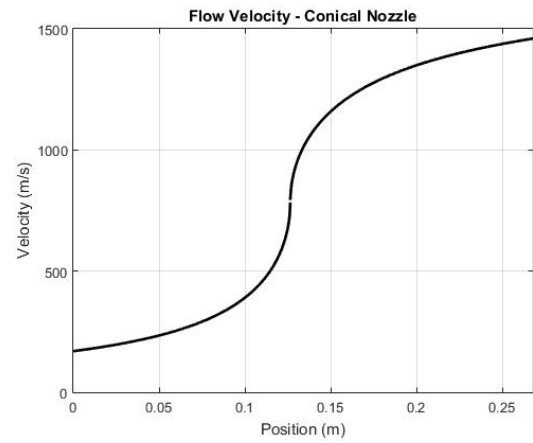


(b) Geometry

Figure 15 – Bell-Shaped Parameters 3

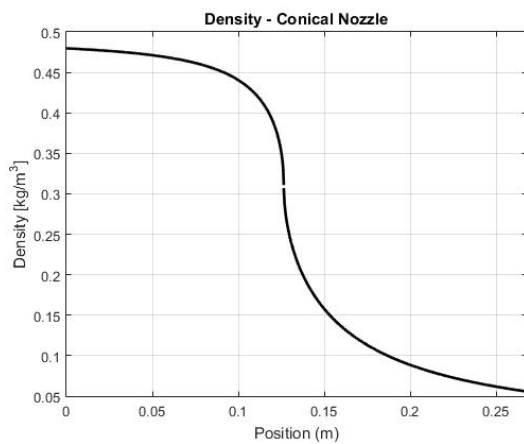


(a) Mach Number

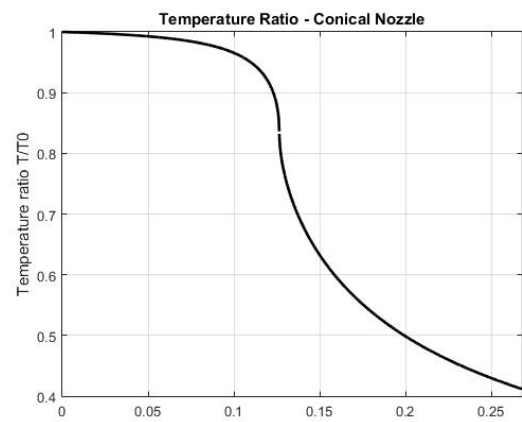


(b) Velocity

Figure 16 – Conical-Shaped Parameters 1



(a) Density



(b) Temperature

Figure 17 – Conical-Shaped Parameters 2

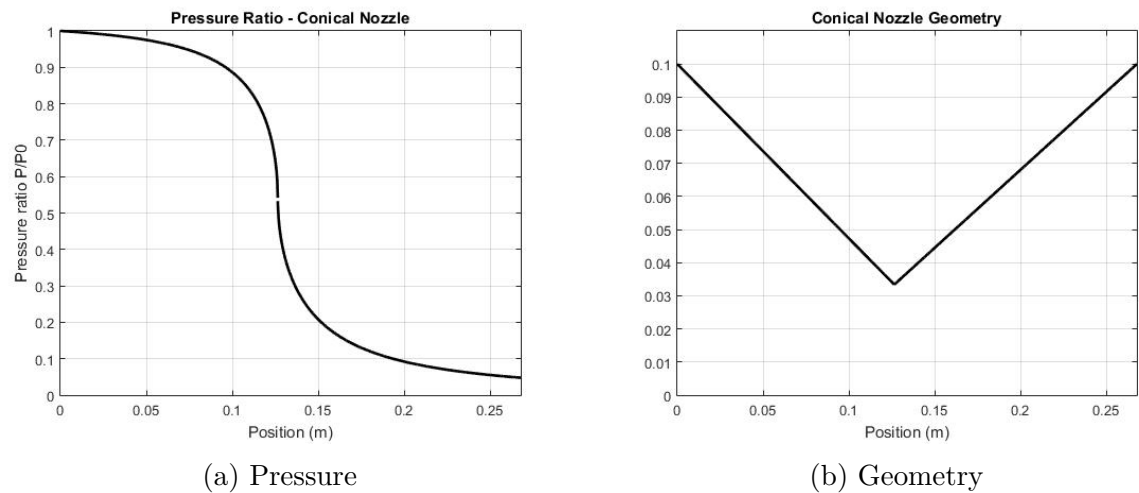


Figure 18 – Conical-Shaped Parameters 3

To compare both geometries, the following Figures (19 to 24) represent the comparison of the properties inside the nozzle in each case.

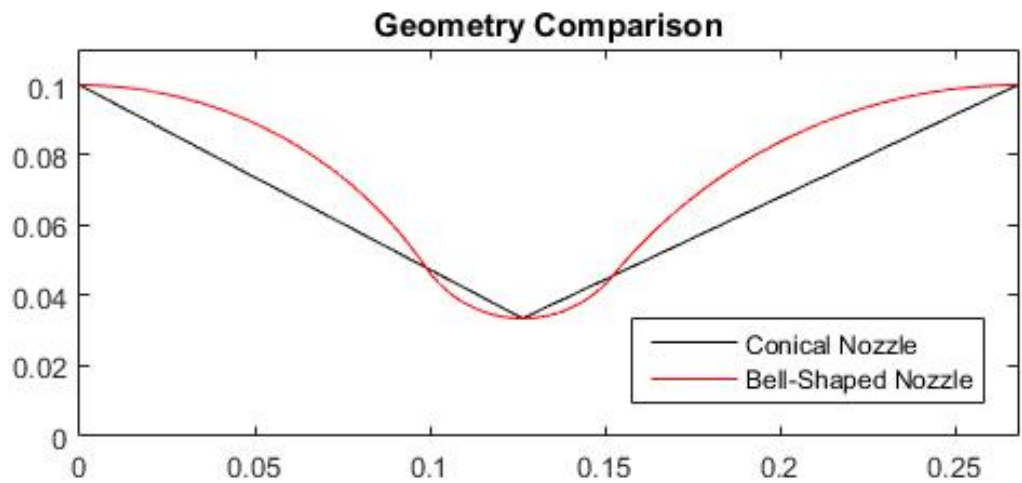


Figure 19 – Geometric Comparison between Nozzles

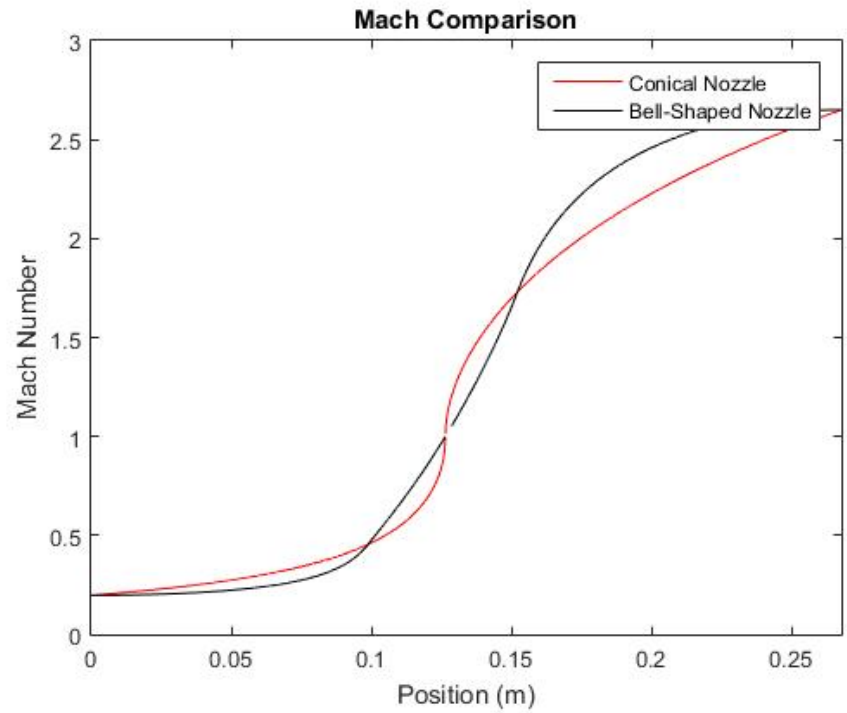


Figure 20 – Mach Number Comparison

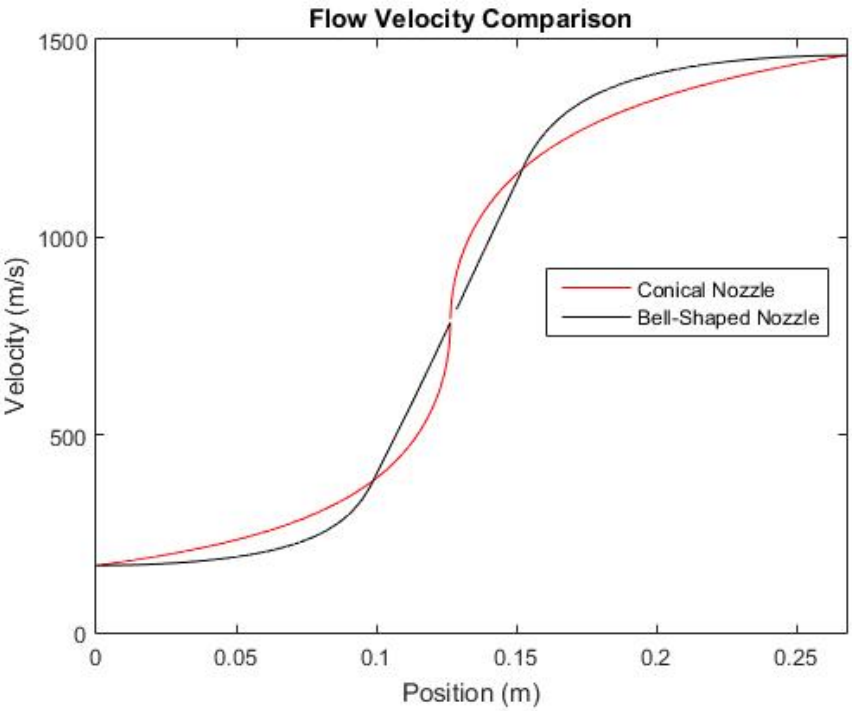


Figure 21 – Flow Velocity Comparison

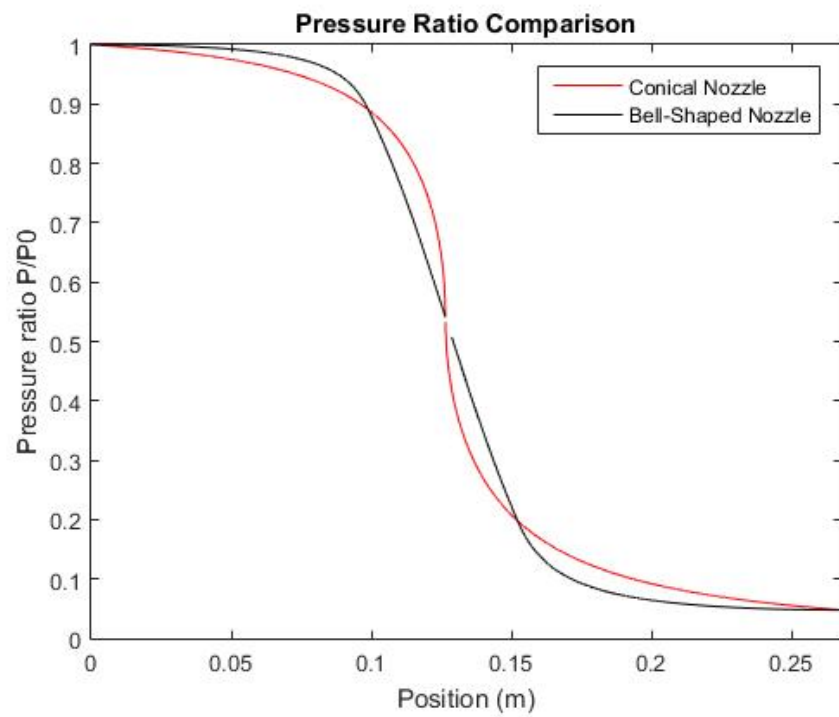


Figure 22 – Pressure Ratio Comparison

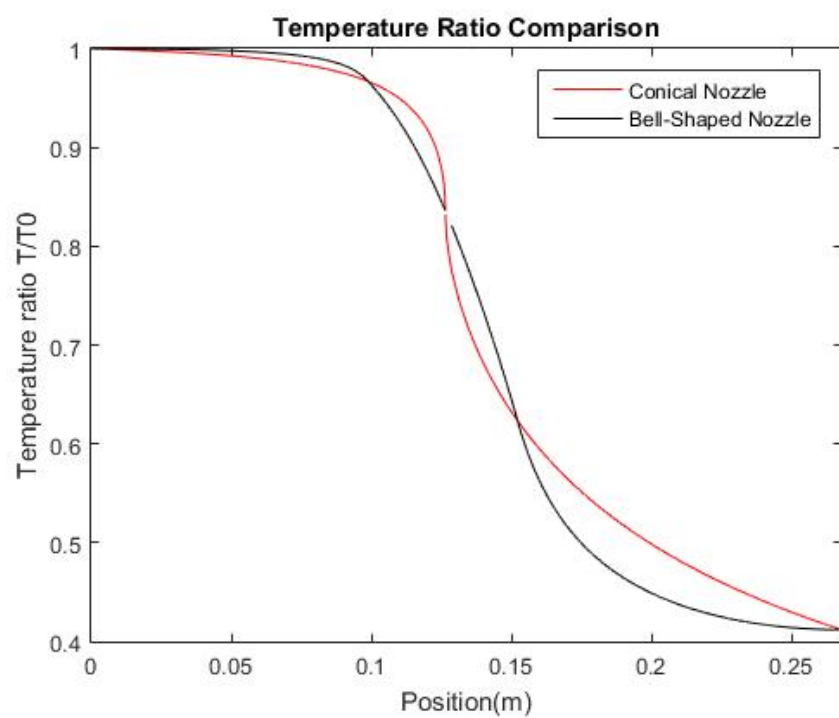


Figure 23 – Temperature Ratio Comparison

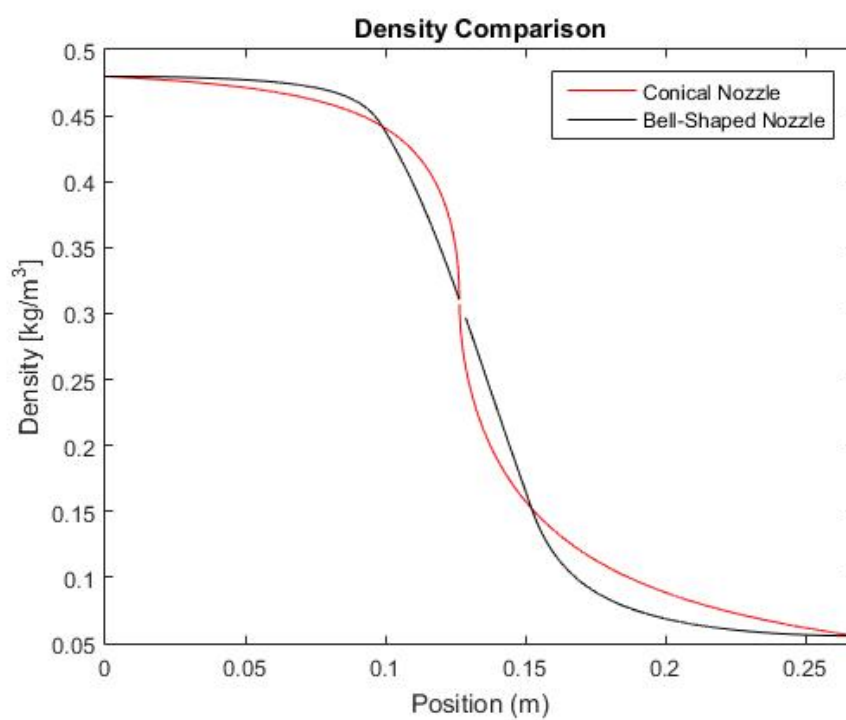


Figure 24 – Density Ratio Comparison

For design purposes, the geometries with their respective measurements were drafted with assistance of CATIA R5V19 with the parameters obtained from the calculations.

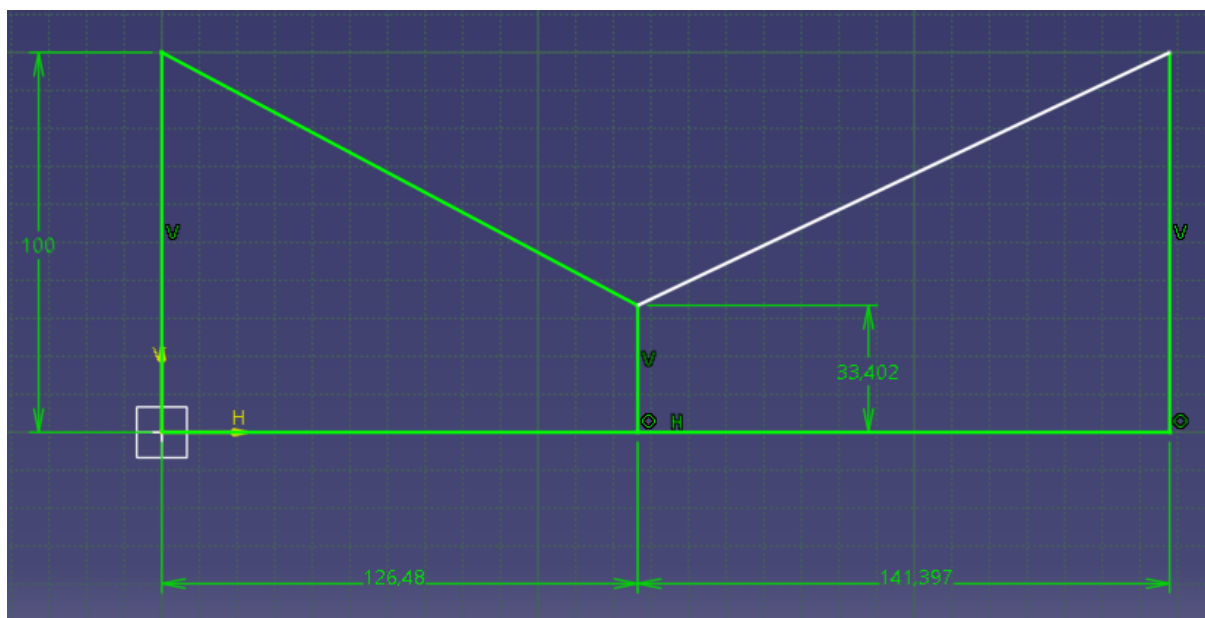


Figure 25 – Conical-Shaped Nozzle

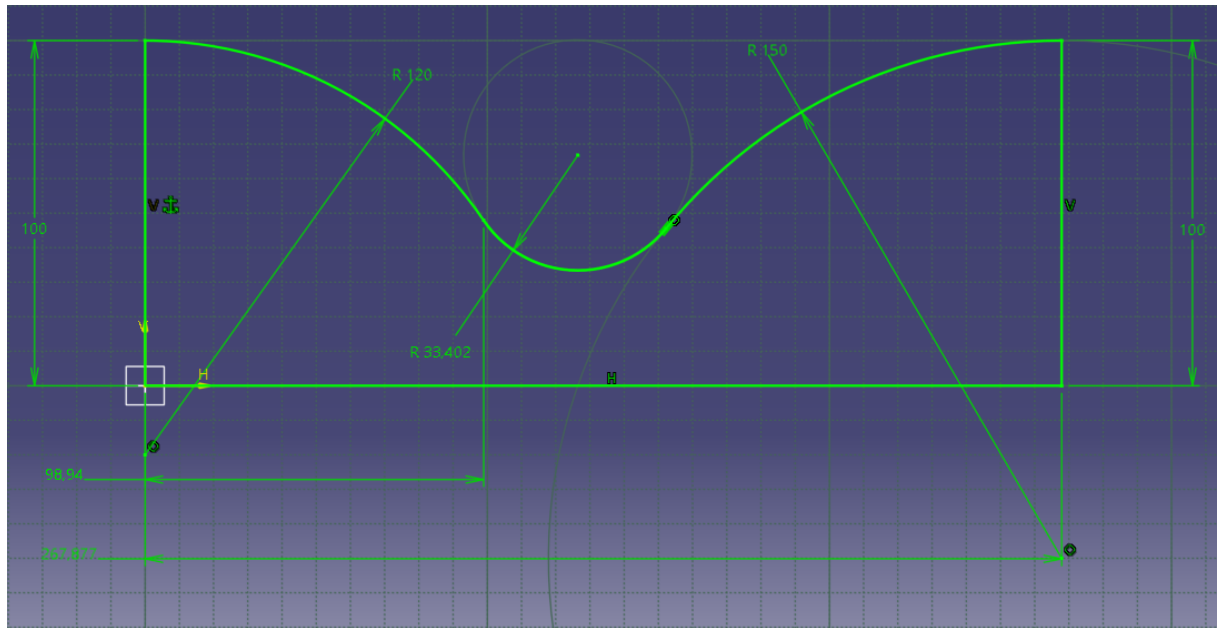


Figure 26 – Bell-Shaped Nozzle

10 Conclusion

A general good result was obtained from the simulations presented in this work. All properties had an expected behavior from what was provided by theory.

In the case of the comparison, what could be observed was that the bell-shaped geometry had the main advantage. First, the changing flow properties from subsonic to supersonic are way more smoother inside the transonic region when compared with the behavior inside conical-shaped.

The flow properties at any x station obtained from the quasi-one-dimensional analysis represents an average of the flow over the given nozzle cross section.

Unfortunately, in view of the simplicity associated with the quasi-one-dimensional theory, it is not possible to predict the details of the actual three-dimensional flow in a convergent-divergent nozzle and it gives no information on the proper wall contour of such nozzles.

From a numerical methods' perspective, in the case of the conical-shaped geometry, only a thin region located next the discontinuity part of the nozzle experienced the throat effect on the flow while for the bell-shaped the situation was more favourable to this compression, which could lead in shock losses inside the nozzle.

All in all, the design of a bell-shaped nozzle can be more sophisticated than an older conical-shaped one.

References

ANDERSON, J. D. *Fundamentals of Aerodynamics*. 5. ed. New York, United States of America: McGraw-Hill Education, 2010. 1106 p. ISBN 978-0-073-39810-5. Cited 7 times in pages [6](#), [7](#), [8](#), [11](#), [19](#), [20](#), and [21](#).

CLARKE, C.; CARSWELL, B. *Principles of Astrophysical Fluid Dynamics*. 1. ed. New York, United States of America: Cambridge University Press, 2007. 226 p. ISBN 978-0-521-85331-6. Cited in page [19](#).

LIEPMANN, H. W.; ROSHKO, A. *Elements of Gasdynamics*. 3. ed. California, United States of America: John Wiley, 2001. 464 p. ISBN 978-0-486-41963-3. Cited 2 times in pages [5](#) and [6](#).

Annex

ANNEX A – Diffuser Design

```

% Atmospheric conditions @ 22km
clc; close all
[T, a, P, rho] = atmosisa(22000);
M1 = 3.5;      %Mach Number

%Free-stream conditions

R = 287;      %Air gas constant [J kg-1 K-1]
P1 = P;       %Free-stream pressure [Pa = N/m2]
T1 = T;       %Free-stream temperature [K]
rho1 = rho;   %Free-stream density [kg/m3]
a1 = a;       %Speed of sound [m/s]
V1 = M1*a1;   %Free-stream velocity [m/s]
g = 1.41203;  %Adiabatic coefficient

P01 = P1*((1+(g-1)/2*M1^2)^(g/(g-1))); %Total pressure
cp = (g*R)/(g-1); %1004.5 [J kg-1 K-1];

Pm = 0;       %loop variable

l1 = .111994;
l2 = .029684;

for beta1 = 1:1:89 %accuracy criteria
    Mn1 = M1*sind(beta1);% sin (degrees)
    Mn2 = sqrt((1+((g-1)/2)*(Mn1^2))/(g*Mn1^2-((g-1)/2)));
    rho2 = rho1*((g+1)*(Mn1^2))/(2+(g-1)*Mn1^2);
    theta1 = atand((2*cotd(beta1)*((M1^2)*(sind(beta1))^2)-1))/...
        ((M1^2)*(g+cosd(2*beta1))+2)); %atand -> degrees;
    M2 = Mn2/sind(beta1-theta1);
    P2 = P1*(1+(2*g/(g+1))*(Mn1^2-1));
    T2 = T1*(P2/P1*rho1/rho2);
    ds = cp*log(T2/T1)-R*log(P2/P1); %log -> ln function;
    P02 = P01*exp(-ds/R);

```

```

a2  = sqrt(g*R*T2);
V2  = M2*a2;

for beta2 = 1:1:89 %accuracy criteria;
    Mn2 = M2*sind(beta2);% sin (degrees)
    Mn3 = sqrt((1+((g-1)/2)*(Mn2^2))/(g*(Mn2^2)-...
        ((g-1)/2)));
    rho3 = rho2*((g+1)*(Mn2^2))/(2+(g-1)*Mn2^2);
    theta2 = atand((2*cotd(beta2)*((M2^2)*sind(beta2)^2-1))/...
        ((M2^2)*(g+cosd(2*beta2))+2)); %atand -> degrees;
    M3 = Mn3/sind(beta2-theta2);
    P3 = P2*(1+(2*g/(g+1))*(Mn2^2-1));
    T3 = T2*(P3/P2*rho2/rho3);
    ds = cp*log(T3/T2)-R*log(P3/P2); %log -> ln function;
    P03 = P02*exp(-ds/R);
    a3 = sqrt(g*R*T3);
    V3 = M3*a3;

```

```

beta3 = 90;

```

```

Mn3 = M3*sind(beta3);% sin (degrees)
Mn4 = sqrt((1+((g-1)/2)*(Mn3^2))/(g*(Mn3^2)-((g-1)/2)));
rho4 = rho3*((g+1)*(Mn3^2))/(2+(g-1)*Mn3^2);
M4 = Mn4;
P4 = P3*(1+(2*g/(g+1))*(Mn3^2-1));
T4 = T3*(P4/P3*rho3/rho4);
ds = cp*log(T4/T3)-R*log(P4/P3); %log -> ln function;
P04 = P03*exp(-ds/R);
a4 = sqrt(g*R*T4);
V4 = M4*a4;

```

```

% Constraint

```

```

if (Pm < P04 && Mn1>=1 && Mn2>=1 && M3>=1)
    Pm = P04;
    opt_M = [M1 M2 M3 M4];
    opt_P = [P1 P2 P3 P4];
    opt_T = [T1 T2 T3 T4];

```

```

    opt_a = [a1 a2 a3 a4];
    opt_V = [V1 V2 V3 V4];
    opt_rho = [rho1 rho2 rho3 rho4];
    opt_P0 = [P01 P02 P03 P04];
    opt_theta = [theta1 theta2];
    opt_beta = [beta1 beta2 beta3];
    n = P04/P01;
    D = 2*l1*sind(theta1)*(P2-P1)+2*l2*sind(theta2)*(P3-P2);
end
end
end

figure(1)
x1 = 0:3;
plot(x1,opt_M)
hold on;
plot(x1,opt_M,'rd');

title('Mach number Variation');
xlabel('Station');
ylabel('Mach Number');
set(gca,'XTick',0:4)

figure(2)
plot(x1,opt_P)
hold on
plot(x1,opt_P,'rd');

title('Pressure Variation');
xlabel('Station');
ylabel('Pressure [Pa]');
set(gca,'XTick',0:3)

figure(3)
plot(x1,opt_T)
hold on
plot(x1,opt_T,'rd');
```

```
title ( 'Temperature Variaton ');
xlabel ( 'Station ');
ylabel ( 'Temperature [K] ');
set ( gca , 'XTick' , 0:3)
```

```
figure (4)
plot (x1,opt_V)
hold on
plot (x1,opt_V, 'rd');
```

```
title ( 'Velocity Variation ');
xlabel ( 'Station ');
ylabel ( 'Velocity [m/s] ');
set ( gca , 'XTick' , 0:3)
```

```
figure (5)
plot (x1,opt_rho)
hold on
plot (x1,opt_rho, 'rd');
```

```
title ( 'Density Variation ');
xlabel ( 'Station ');
ylabel ( 'Density [kg/m^3] ');
set ( gca , 'XTick' , 0:3)
```

ANNEX B – Nozzle Design

```

clear; clc; close all;
format long

%Properties in the exit of the diffuser
T3 = 701.21121;           %Temperature
                             %(T)    [K]
P3 = 189115.270458306;    %Pressure
                             %(P)    [Pa]
M3 = 0.656150437410476;   %Mach Number
                             %(M)
rho3 = 0.939541230625329; %Density
                             %(rho)  [kg/m^3]
D = 100/1000;             %External Diameter
                             %(D)    [mm]
Din = (100-24.368)/1000;  %Internal Diameter
                             %(Din)  [mm]
d3 = (D-Din);             %Diameter
                             %(d)    [m]
A3 = d3*1;                %Area for unit span wedge surface
                             %(A)    [m^2]

g = 1.41203;              %Degrees of freedom in a gas (gamma)
R = 287;                  %Gas Universal Constant [J*Kg^-1*K^-1]

a3 = sqrt(g*R*T3);        %Sound Speed [m/s]
u3 = a3*M3;               %Flow Velocity [m/s]

%Throat Area Auxiliar -> To evaluate the Mach Number after Expansion

Aaux = A3/sqrt((1/M3^2)*(((2)/(g+1))*...
(1+((g-1)/2)*M3^2))^(((g+1)/(g-1)))));

%Stagnation Properties in Volume 3

```

```

T0aux    = T3*(1+((g-1)/2)*M3^2);
P0aux    = P3/(1+((g-1)/2)*M3^2)^(-g/(g-1));
rho0aux  = rho3*((1+((g-1)/2)*M3^2)^(1/(g-1)));

```

```
%Properties in Volume 4 (Total properties stay the same)
```

```
A4      = 0.1;
```

```

f        = @(M4) ((A4/Aaux)^2 - 1/M4^2 * (2/(g+1) * (1 + (g-1)...
                * M4^2 /2)))^( -(g+1)/(g-1));
M4       = fzero(f,0.01,3);
T4       = T0aux/(1+((g-1)/2)*M4^2);
P4       = P0aux*((1+(g-1)/2)*M4^2)*(-g/(g-1));
rho4     = rho0aux/((1+((g-1)/2)*M4^2)^(1/(g-1)));
a4       = sqrt(g*R*T4);
u4       = M4*a4;

```

```
%Heat addition (4-5)
```

```

P04      = P0aux;
T04      = T0aux;
T5       = T4+1000;

```

```
%Properties in Volume 5
```

```
A5 = A4;
```

```

f        = @(M5) T5/T4 - (((1+g*M4^2)/(1+g*M5^2))^2)*((M5/M4)^2);
M5       = fzero(f,M4);
P05      = P04* ((1+g*M4^2)/(1+g*M5^2))...
            *((1+((g-1)/2)*M5^2)/(1+((g-1)/2)*M4^2))^(g/(g-1));
T05      = T04*((1+g*M4^2)/(1+g*M5^2))...
            *((1+((g-1)/2)*M5^2)/(1+((g-1)/2)*M4^2))*(M5/M4)^2;
rho5     = rho4*(((1+g*M5^2)/(1+g*M4^2)))*(M4/M5)^2;
rho05    = rho5*(1+((g-1)/2)*M5^2)^(1/(g-1));
P5       = P4*((1+g*M4^2)/(1+g*M5^2));
a5       = sqrt(R*g*T5);

```

```

u5      = M5*a5;

%Properties in Volume 6

A6      = A5/sqrt((1/M5^2)*(((2/(g+1)))*(1+((g-1)/2)*M5^2))^(((g+1)/(g-1))));

Dt = A6/1;                                %Area per unit span

%Calculating distances

x_t = sqrt((1.2*D+Dt)^2-(2*Dt+0.2*D)^2);
x_t2 = sqrt((1.5*D+Dt)^2-(2*Dt+0.5*D)^2)+x_t;

% Geometric Shapes

[xb,Rb_x,Mb_x,Pb_x,Tb_x,rhob_x,ub_x] = bell_geometry...
                                      (x_t,x_t2,Dt,P05,T05,rho05,A6);

[xc,Rc_x,Mc_x,Pc_x,Tc_x,rhoc_x,uc_x] = conical_geometry...
                                      (x_t,x_t2,Dt,P05,T05,rho05,A6);

% Comparisons

figure(13);
plot(xc,Rc_x,'k'); axis equal;
hold on
plot(xb,Rb_x,'r');
title('Geometry Comparison')
legend('Conical Nozzle','Bell-Shaped Nozzle');
ylim([0,0.11]);
xlim([0 xc(end)]);

figure(14)
plot(xc,Mc_x,'r');
hold on
plot(xb,Mb_x,'k');
title('Mach Comparison')
xlabel('Position (m)');

```



```

ylabel('Mach Number');
legend('Conical Nozzle','Bell-Shaped Nozzle');
xlim([0 xc(end)]);

```

```

figure(15);
plot(xc,Pc_x/Pc_x(1),'r');
hold on;
plot(xb,Pb_x/Pb_x(1),'k');
title('Pressure Ratio Comparison');
xlabel('Position (m)');
ylabel('Pressure ratio P/P0');
legend('Conical Nozzle','Bell-Shaped Nozzle');
xlim([0 xc(end)]);

```

```

figure(16);
plot(xc,Tc_x/Tc_x(1),'r');
hold on;
plot(xb,Tb_x/Tb_x(1),'k');
title('Temperature Ratio Comparison');
ylabel('Temperature ratio T/T0');
xlabel('Position(m)');
legend('Conical Nozzle','Bell-Shaped Nozzle');
xlim([0 xc(end)]);

```

```

figure(17);
plot(xc, rhoc_x,'r');
hold on
plot(xb, rhob_x,'k');
title('Density Comparison');
ylabel('Density [kg/m^3]');
xlabel('Position (m)');
legend('Conical Nozzle','Bell-Shaped Nozzle');
xlim([0 xc(end)]);

```

```

figure(18)
plot(xc,uc_x,'r');
hold on
plot(xb,ub_x,'k');
title('Flow Velocity Comparison');

```

```
xlabel('Position (m)');  
ylabel('Velocity (m/s)');  
legend('Conical Nozzle','Bell-Shaped Nozzle');  
xlim([0 xc(end)]);
```

ANNEX C – Bell-Shaped Parameters

```

function [xb,Rb_x,Mb_x,Pb_x,Tb_x,rhob_x,ub_x] = bell_geometry ...
    (x_t,x_t2,Dt,P05,T05,rho05,A6)

g      = 1.41203;                %Degrees of freedom in a gas (gamma)
R      = 287;                    %Gas Universal Constant [J*Kg-1*K-1]

%Auxiliar function to round numbers
roundn = @(x,n) round(x.*10.^n)./10.^n;

%Bell Shaped Geometry

x1 = 0:0.00001:0.09894;          %Geometric Restriction
x2 = x1(end):0.00001:0.152232;   %Geometric Restriction
x3 = x2(end):0.00001:roundn(x_t2,5);
xb = [x1 x2 x3];

Rb_x1 = sqrt(0.12^2-(x1-0).^2)-0.02;
Rb_x2 = -sqrt(Dt^2-(x2-x_t).^2)+2*Dt;
Rb_x3 = sqrt(0.15^2-(x3-x_t2).^2)-0.05;
Rb_x = [Rb_x1 Rb_x2 Rb_x3];

Ab_x = Rb_x;
Mb_x = zeros(length(Ab_x),1);

%Mach at subsonic region

for i=1:find(Ab_x==min(Ab_x))
    A_x = Ab_x(i);
    f = @(Mb_x) ((A_x/A6).^2 - 1/Mb_x.^2 * (2/(g+1) * (1 + (g-1)...
        * Mb_x.^2 /2)).^( (g+1)/(g-1)));
    Mb_x(i) = fzero(f,1);
end

%Mach at supersonic region

```

```

for i = find(Ab_x == min(Ab_x)): length(Ab_x)
    A_x = Ab_x(i);
    f = @(Mb_x) ((A_x/A6).^2 - 1/Mb_x.^2 * (2/(g+1) * (1 + (g-1)...
        * Mb_x.^2 / 2)).^( (g+1)/(g-1)));
    Mb_x(i) = fzero(f,10);
end

%Properties
Pb_x = P05*(1+(g-1)*Mb_x.^2/2).^(-g/(g-1));
Tb_x = T05*(1+(g-1)*Mb_x.^2/2).^(-1);
rhob_x = rho05./((1+((g-1)/2)*Mb_x.^2).^(1/(g-1)));
ab_x = sqrt(g*R*Tb_x);
ub_x = ab_x.*Mb_x;

figure(1);
plot(xb,Rb_x,'r','LineWidth',2);
ylim([0 0.11]);
title('Bell Shaped Nozzle Geometry');
xlabel('Position (m)');
xlim([0 xb(end)]);
grid on

figure(2);
plot(xb,Mb_x,'r','LineWidth',2);
title('Mach Number - Bell Shaped Nozzle');
xlabel('Position (m)');
ylabel('Mach number M');
xlim([0 xb(end)]);
grid on

figure(3);
plot(xb,Pb_x/Pb_x(1),'r','LineWidth',2);
title('Pressure Ratio - Bell Shaped Nozzle');
xlabel('Position (m)');
ylabel('Pressure ratio P/P0');
xlim([0 xb(end)]);
grid on

```

```
figure(4);
plot(xb, Tb_x/Tb_x(1), 'r', 'LineWidth', 2);
title('Temperature Ratio – Bell Shaped Nozzle');
ylabel('Temperature ratio T/T0');
xlabel('Position (m)');
xlim([0 xb(end)]);
grid on
```

```
figure(5);
plot(xb, rhob_x, 'r', 'LineWidth', 2);
title('Density – Bell Shaped Nozzle');
ylabel('Density [kg/m3]');
xlabel('Position (m)');
xlim([0 xb(end)]);
grid on
```

```
figure(6);
plot(xb, ub_x, 'r', 'LineWidth', 2);
title('Flow Velocity – Bell Shaped Nozzle');
xlabel('Position (m)');
ylabel('Velocity (m/s)');
xlim([0 xb(end)]);
grid on
```

```
end
```

ANNEX D – Conical-Shaped Parameters

```

function [xc,Rc_x,Mc_x,Pc_x,Tc_x,rhoc_x,uc_x] = conical_geometry...
    (x_t,x_t2,Dt,P05,T05,rho05,A6)

g      = 1.41203;                %Degrees of freedom in a gas (gamma)
R      = 287;                    %Gas Universal Constant [J*Kg-1*K-1]
D      = 0.1;                    %External Diameter

%Auxiliar function to round numbers
roundn = @(x,n) round(x.*10.^n)./10.^n;

xc1 = 0:0.00001:x_t;
xc2 = x_t:0.00001:roundn(x_t2,5);
xc  = [xc1 xc2];

Rc_x1 = (Dt-D)/x_t*xc1+D;
Rc_x2 = (D-Dt)/(xc(end)-xc2(1))*(xc2 - xc2(1))+ Dt;
Rc_x  = [Rc_x1 Rc_x2];

Ac_x = Rc_x;
Mc_x = zeros(length(Ac_x),1);

%Subsonic Region

for i = 1:find(Ac_x == min(Ac_x))
    A_x = Ac_x(i);
    f = @(Mc_x) ((A_x/A6).^2 - 1/Mc_x.^2 * (2/(g+1) * (1 + (g-1)...
        * Mc_x.^2 /2)).^( (g+1)/(g-1)));
    Mc_x(i) = fzero(f,1);
end

%Supersonic Region

for i = find(Ac_x ==min(Ac_x)): length(Ac_x)
    A_x = Ac_x(i);
    f = @(Mc_x) ((A_x/A6).^2 - 1/Mc_x.^2 * (2/(g+1) * (1 + (g-1)...

```

```

        * Mc_x.^2 /2)).^( (g+1)/(g-1)));
    Mc_x(i) = fzero(f,10.5);
end

%Properties
Pc_x = P05*(1+(g-1)*Mc_x.^2/2).^(-g/(g-1));
Tc_x = T05*(1+(g-1)*Mc_x.^2/2).^(-1);
rhoc_x = rho05./((1+(g-1)/2*Mc_x.^2).^(1/(g-1)));
ac_x = sqrt(g*R*Tc_x);
uc_x = ac_x.*Mc_x;

%Plot

figure(7);
plot(xc,Rc_x,'k','LineWidth',2);
ylim([0 0.11]);
xlim([0 0.258]);
title('Conical Nozzle Geometry');
xlabel('Position (m)');
xlim([0 xc(end)]);
grid on

figure(8);
plot(xc,Mc_x,'k','LineWidth',2);
title('Mach Number - Conical Nozzle');
xlabel('Position (m)');
ylabel('Mach Number M');
xlim([0 xc(end)]);
grid on

figure(9);
plot(xc,Pc_x/Pc_x(1),'k','LineWidth',2);
title('Pressure Ratio - Conical Nozzle');
xlabel('Position (m)');
ylabel('Pressure ratio P/P0');
xlim([0 xc(end)]);
grid on

figure(10);

```

```
plot(xc,Tc_x/Tc_x(1),'k','LineWidth',2);  
title('Temperature Ratio – Conical Nozzle');  
ylabel('Temperature ratio T/T0');  
xlim([0 xc(end)]);  
grid on
```

```
figure(11);  
plot(xc,rhoc_x,'k','LineWidth',2);  
title('Density – Conical Nozzle');  
ylabel('Density [kg/m3]');  
xlabel('Position (m)');  
xlim([0 xc(end)]);  
grid on;
```

```
figure(12);  
plot(xc,uc_x,'k','LineWidth',2);  
title('Flow Velocity – Conical Nozzle');  
xlabel('Position (m)');  
ylabel('Velocity (m/s)');  
xlim([0 xc(end)]);  
grid on
```